# Original Paper

## Evaporation in industrial glass melt furnaces

Ruud G. C. Beerkens

Eindhoven University of Technology, Eindhoven (The Netherlands)

Johannes van Limpt

TNO Institute of Applied Physics (TPD), Eindhoven (The Netherlands)

Process conditions in glass furnaces, especially the settings of the combustion system, determine the rate of the evaporation processes at the glass melt surface. Reduction of volatilization to lower dust and heavy metal emissions, to minimize the refractory attack by the aggressive volatile components, and to limit depletion of volatile glass components at the glass melt surface is of great technological importance. This can be achieved by changes in burner design and burner positioning, optimizing combustion control and avoiding extreme glass surface temperatures. Such high local temperatures at the glass surface may lead to very high concentrations of PbO, NaOH or KOH vapors attacking the crown materials of the furnace.

Evaporation model studies show the potential of process measures for the reduction of evaporation and minimizing depletion of alkali, lead or boron compounds at the glass melt surface. Sodium depletion down to 80 % of the original content can take place at the glass melt surface, in lead silicate melting processes depletion may reduce the lead concentrations by more than 50 %. Industrial tests support the results of modeling studies and show the effects of the settings of the combustion processes on glass-melt evaporation kinetics.

**Verdampfung in industriellen Glasschmelzöfen**

Die Prozeßbedingungen im Glasschmelzofen, insbesondere die des Verbrennungsprozesses, bestimmen die Kinetik der Verdampfung an der Glasschmelzoberfläche. Eine Minderung der Verdampfung zur Reduktion von Staub- und Schwermetallemissionen, zum Schutz des Feuerfestmaterials und zur Vermeidung von Glaskomponentenverarmung an der Glasoberfläche kann durch Änderungen in der Brennerkonstruktion, in der Brennerpositionierung und in der Brennersteuerung (Brennstoff–Luft- oder Brennstoff–Sauerstoff-Verhältnis) realisiert werden. Extrem hohe Temperaturen an der Oberfläche der Schmelze ergeben lokal sehr hohe Verdampfungsraten sowie hohe PbO-, NaOH- und KOH-Konzentrationen im Oberofen, die das Gewölbe gefährden.

Bei einer starken Verdampfung kann eine Verarmung des $Na_2O$-Gehaltes an der Oberfläche der Schmelze auftreten, wobei die $Na_2O$-Konzentration bis auf 80 % des Gehaltes in der Grundglasschmelze absinken kann. In Bleiglaswannen ist eine Verarmung des PbO-Gehaltes an der Glasschmelzoberfläche von bis zu 50 % möglich. Studien mit Hilfe von Verdampfungsmodellen zeigen die primären Möglichkeiten zur Verminderung der Verdampfung. Ergebnisse industrieller Testversuche in der Glasindustrie stimmen mit Modellvorhersagen überein und zeigen die Effekte der Verbrennungsparameter auf die Verdampfung und die Staubemissionen.

### 1. Introduction

Evaporation of contaminants in the glass-forming batch or volatilization of glass melt components lead to:

- emissions of heavy metals or submicron-sized dust often requiring the installation of filter systems [1];
- refractory attack by aggressive volatile components such as alkali vapors (NaOH, NaCl, KOH, KCl, LiOH) or lead components (Pb, PbO) [2];
- fouling and plugging of the regenerator checker work, flue gas channels or waste heat boilers by deposits containing evaporated glass constituents [3 to 5];
- depletion of volatile glass components at the glass melt surface, causing cord in the final product, examples are lead and fluoride depletion [6 and 7] or the formation of boron-lean, silica-rich knots in borosilicate glasses [8];
- loss of expensive components such as boron and lead compounds, where recycling of the collected filter dusts will compensate for these losses.

The superstructure attack by glass melt vapors has frequently been observed soon after the application of

Received 5 July 2001.

Presented in German at: 75st Annual Meeting of the German Society of Glass Technology (DGG) in Wernigerode on 23 May 2001.

oxygen combustion technology in glass furnaces. Due to the much lower combustion-gas volume flows in oxygen–fossil fuel combustion processes compared to air firing, the evaporated components become much less diluted in the furnace atmosphere and the higher vapor pressures of alkali or lead components increase the potential for silica refractory attack. At high alkali or lead partial vapor pressures, liquid silicates can be formed at the lower end of the crown temperature levels, especially in joints and in the doghouse area. Faber [2] shows that silica refractory materials are mainly applicable in a certain temperature range, below a minimum temperature alkali reacts with silica and above a maximum level silica will show creep and starts to deform. The width of the temperature window for silica use in glass furnaces depends on the concentration of alkali or lead vapors. At high concentration levels the minimum allowable temperature shifts to higher values and the temperature window becomes smaller.

The dust collected by filters or emitted through the chimney contains mainly the most volatile components of the glass composition such as: $Na_2O$, $K_2O$, $B_2O_3$, PbO, $Sb_2O_3$, chlorides, sulfates. In most glass furnaces, these dust particles are submicron-sized (mainly single particle diameters of 0.03 to 0.5 μm) [9] and are airborne, obtained from condensation processes during the cooling of the flue gases. Table 1 shows the ranges of compositions of filter dust collected from different industrial glass furnaces. The small raw material particles from the batch (> 10 μm) deposit mainly at the top layer of the regenerator checkers or in the high-temperature inlet sections of the recuperators. Only a very small part of the carry-over will reach the chimney or filter system. Material balances show that in common soda–lime–silica furnaces, the regenerators collect only 3 to 5 % of the flue gas condensation products.

In this paper the most important vapor species, originating from the batch or glass melt will be given and the mechanisms of evaporation are discussed. A simulation model description for the evaporation process of alkali compounds from soda–lime–silica melts (typical for container and float glasses) will be presented and results of some model calculations will be shown here. Recommendations for the reduction of evaporation rates and consequently minimizing refractory attack by volatile components of the glass melt will be derived from the model studies. The impact of adjustments of the combustion processes in industrial furnaces on the evaporation of alkali compounds will be demonstrated and the results of these industrial tests are also compared with modeling results.

## 2. Mechanisms of evaporation from glass melt surfaces

During the glass melting process, part of the melt will be exposed to hot strongly flowing combustion gases at the glass melt surface. During this time of exposure, volatile glass components may evaporate from the melt by:

a) direct evaporation of the volatile component without any chemical reaction at the surface of the melt, an example is PbO evaporation from lead silicate melts.

b) Evaporation by a chemical reaction of a glass melt component at the glass surface with a gas species in the combustion space, examples are the evaporation of NaOH due to a reaction of $Na_2O$ from the melt and water vapor [10 to 14], generated from the combustion process or due to reduction of $Na_2O$ by reducing gases such as CO:

$$Na_2O\,(melt) + CO \Rightarrow Na\,(gas) + CO_2\,. \qquad (1)$$

c) a reaction between two glass melt components, forming a compound with a high chemical activity in the melt or a high vapor pressure; an example is the formation of highly volatile alkali meta-borates ($NaBO_2$ or $KBO_2$) from $Na_2O$ or $K_2O$ and $B_2O_3$ in alkali–borosilicate melts [14 to 17].

The incongruent evaporation processes from multicomponent silicate melts has been investigated by many researchers [10 to 24]. Depletion of the volatile component at the glass melt surface is often observed in borosilicate or lead silicate glass melting furnaces [6 to 8]. This depletion is often caused by very high vapor pressures and high evaporation rates on the one hand and on the other hand, limited borium oxide or lead oxide diffusion mass transfer from the bulk of the melt to the glass surface.

The rate of evaporation of a certain glass melt component is governed by the following sequence of steps:

- Diffusion of the volatile component from the bulk of the melt to the surface of a generally almost static (non-stirred) glass melt surface layer.
- Evaporation or chemical reactions at the surface of the glass melt. In general, the high gas temperatures ensure that reaction kinetics is very fast compared to the diffusion rates and a local chemical equilibrium at the glass melt surface may be assumed: the vapor pressures of evaporated species at the surface are in equilibrium with the concentrations of volatile glass components in the surface glass composition.
- Diffusion of the evaporating species through an almost static gaseous boundary layer above the melt. The diffusion mass transfer increases as the thickness of this boundary layer reduces due to larger gas velocities. The diffusion rate also depends on the difference of the partial vapor pressures of the evaporating species between the surface of the melt and in the main gas stream in the combustion space.

For moderate gas velocities and relatively low temperatures, diffusion in the melt compensates almost completely for the evaporation losses at the surface. Then, the evaporation rate and loss is governed by the diffusion in the gas phase. However, at higher evaporation

Table 1. Typical dust emissions and dust composition of glass furnaces

| | industrial glass furnace for | | | | |
|---|---|---|---|---|---|
| | container glass (regenerative) | float glass (regenerative) | TV panel glass (regenerative) | sodiun boro-silicate glass (recuperative) | E-glass (recuperative) |
| dust concentration[1] in mg/m³ | | | | | |
| | 125 to 200 | 120 to 180 | 200 to 275 | 1500 to 2000 including boric acids | 800 to 1400 including boric acids |
| specific emission in kg/t glass | | | | | |
| | 0.17[2] to 0.4 | 0.3 to 0.45 | 0.5 to 0.9 | 3.5 to 5 including boric acids | 3.0 to 5.0 including boric acids |
| dust composition in wt% | | | | | |
| $Na_2O$ | 25 to 40 | 35 | 12 to 18 | 25 to 30 | 2.0 to 5.0 |
| $K_2O$ | 1.5 to 2.5 | 0 to 1 | 35 to 40 | 5.0 to 10 | 10.0 to 20.0 |
| $SO_3$ | 45 to 55 | 45 to 55 | 5 to 10 | 8.0 to 15 | 2.0 to 5.0 |
| PbO | 0 to 5 | <0.2 | <1 | <0.5 | <0.1 |
| $B_2O_3$ | <1 | <0.1 | – | 35 to 40 | 55 to 70 |
| $Sb_2O_3$ | <0.2 | <0.1 | 8 to 12 | <0.2 | 0 |
| $SiO_2$ | 0.5 to 2 | 0.5 to 1.5 | <5 | <2 | 1.0 to 3.0 |
| $Al_2O_3$ | 0.2 to 1 | <1 | <1 | <2 | <1.5 |
| MgO | 1.0 to 3.0 | 1.0 to 3.0 | <1 | 1.0 to 3.0 | 0 to 1 |
| CaO | 2.0 to 7.0 | 2.5 to 4.0 | <1 | 2.0 to 5.0 | 2 |
| chlorides | <1 | <1 | 5 to 8 | <1 | <1 |
| fluorides | <1 | <1 | 6 to 12 | <1 | <0.25 |
| residue | 5 to 12 | 10 | 10 to 15 | 10 | 5 to 10 |

[1] Based on flue gas volume (dry, 8 % oxygen) of gas–air fired furnaces.
[2] Oxygen-fired furnaces.

rates and for very volatile species such as boron, lead and fluoride compounds, depletion of these components at the glass melt surface can take place. Then, also diffusion in the melt will influence evaporation losses and evaporation rates may become time-dependent for static melts. At the top of a glass melt, the glass melt layer exposed to the furnace atmosphere may become almost static. This is especially the case when the density of the surface glass is lower compared to the parent glass melt and when the surface tension of the parent glass is higher than the surface tension of the melt at the top surface [25].

## 3. Evaporating species

Several publications address the identification or characterization of evaporation species from molten glasses [26 to 31]. Mass spectrometric analysis of high-temperature vapors or thermodynamic modeling [32 and 33] provide information on the possible species existing above glass melts. It is generally accepted that NaOH, NaCl, and at reducing conditions Na, are the dominant sodium species above soda–lime–silica melts, in dry atmospheres also NaO may become relatively important. For borosilicate melts, borates such as $NaBO_2$, $KBO_2$, $HBO_2$ vapors [14, 15, 17, 24 and 30] can be expected. Meta-boric acid ($HBO_2$) is formed by reactions between borates in the melt and water vapor. Lead silicates release PbO, Pb (at reducing conditions) and probably some lead hydroxide species when exposed to water-vapor containing atmospheres. Conradt and Scholze [14] showed the linear increasing lead evaporation losses for a potassium–lead–silicate (20 wt% PbO) melt at increasing water-vapor pressures at temperatures >1100 °C. This might be explained by formation of $Pb(OH)_2$ vapor. Hoheisel and Schaeffer [34], however, found only very moderate influence of the presence of water vapor on the evaporation of lead components from lead silicate melts with more than 70 wt% PbO at temperatures below 1200 °C.

Dependent on the raw materials and the contaminations in the batch, HF, NaF [35] and NaCl [36 and 37] may evaporate from the melt or batch blanket. The use of arsenic or antimony based fining agents will cause evaporation of arsenic or antimony species. At increasing water-vapor pressure ($p_{H2O}$) antimony evaporation will be enhanced proportional to $p_{H2O}^{3/2}$, an indication of the formation of $Sb(OH)_3$ gaseous species. This short

summary of evaporating components shows the important role of water vapor, stimulating NaOH, KOH, $HBO_2$, $Sb(OH)_3$ evaporation and the effect of reducing conditions leading to elemental lead, sodium, potassium evaporation.

## 4. Condensation of vapors

During sulfate decomposition in the fining process, sulfur oxides evolve from the molten glass. These sulfur gases react with other evaporated species during the cooling of the flue gases. The formation of sodium sulfate salts in regenerators is a typical example. Very fine sodium sulfate droplets will be formed below about 1100 °C [4], solidification of these drops into small dust particles takes place below 884 °C. A small part of these condensation products will deposit at the regenerator checker bricks. Sodium sulfate appears to have a very low vapor pressure compared to the NaOH vapor pressures in glass furnaces and after sodium sulfate vapor formation, condensation of this compound occurs. The reactions involved in this fouling mechanism of regenerators are:

$$2\ \mathrm{NaOH\ (gas)} + \mathrm{SO_2} + 1/2\ \mathrm{O_2} \Rightarrow \mathrm{Na_2SO_4\ (liquid/solid)} + \mathrm{H_2O}\ , \quad (2)$$

$$2\ \mathrm{NaCl\ (gas)} + \mathrm{SO_2} + 1/2\ \mathrm{O_2} \Rightarrow \mathrm{Na_2SO_4\ (liquid/solid)} + 2\ \mathrm{HCl}\ . \quad (3)$$

Thus, sodium chloride added to the batch by chlorides in the synthetic soda, or in the cullet leads to extra sodium sulfate formation and extra HCl emissions. Without the use of sulfates in the batch and sulfur-lean fuels, sodium hydroxides evaporating from melts may form NaCl or $Na_2CO_3$ dust and deposits instead of $Na_2SO_4$. In this paper the evaporation of sodium species will be discussed and a simulation model for the prediction of sodium losses from glass melts will be presented here. Similar models can be established for other evaporating compounds.

## 5. Modeling of evaporation losses from glass melt surfaces

The evaporation process from glass melts in industrial glass furnaces can be described as a process of diffusion of a volatile component in an almost static glass melt layer moving along a glass surface exposed to a gas flow or flames over a length $L_g$, typically a few meters. At the glass melt surface, the component j reacts or evaporates, forming volatile component i (vapor pressure $p_i$). This component i diffuses in the boundary layer (1 to 5 cm thickness) in the gas phase above the melt. Figure 1 illustrates this process. In cases of static melts, depletion of component j at the surface layer of the melt will take place, the degree of depletion depends on time, diffusion rate in the melt and the evaporation rate.

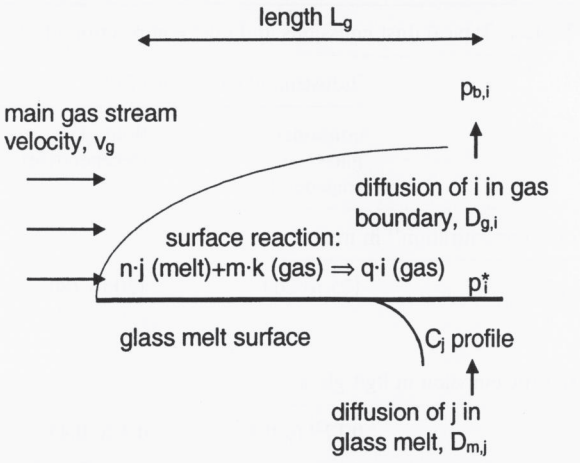


Figure 1. Schematic presentation of evaporation process for a component j from a glass melt exposed to a gas flow with a reacting gas species k.

The diffusion ($D_{m,j}$) of an evaporating glass melt component j to the surface of the glass melt (m) can be described by the second diffusion law of Fick, describing the concentration profile of $C_j$ in the melt:

$$\partial C_j/\partial t = D_{m,j} \cdot \partial^2 C_j/\partial x^2\ . \quad (4)$$

The distance perpendicular to the glass surface is given by the coordinate $x$. At the glass melt surface, at $x = 0$, the loss of component j is given by:

$$Q_j = -\ D_{m,j} \cdot (\partial C_j/\partial x)_{x=0}\ . \quad (5)$$

Matoušek and Hlavac [19], Terai and Ueno [20], and Cable et al. [21] derived the solution of this differential equation, assuming a reaction or mass transfer process at the glass melt surface with a proportionality between the surface concentration of the evaporating component $C_{j,x=0}$ and the evaporation loss rate $Q_j$:

$$Q_j = h \cdot C_{j,x=0}\ . \quad (6)$$

The value of $h$ is mainly dependent on the saturation vapor pressures of all volatile components containing the glass component j and the diffusion mass transfer process in the gaseous boundary layer. The saturation vapor pressure is dependent on the glass composition at the surface.

Evaporation of a component j from the melt reacting with a gas k and forming gaseous species i according, to

$$n \cdot \mathrm{j\ (melt)} + m \cdot \mathrm{k\ (gas)} \Leftrightarrow q \cdot \mathrm{i\ (gas)} \quad (7)$$

leads to loss of glass component j. For ideal conditions the saturation pressure of component i ($p_i^*$) depends on the concentration of component j at the glass melt surface:

$$p_i^{*q} = K(T) \cdot C_j^n \cdot p_k^m \,. \tag{8}$$

$K(T)$ is a temperature-dependent equilibrium constant and $p_k$ is the partial pressure of reacting gas components ($p_{H2O}$ or $p_{CO}$).

The local loss of component j (for instance $Na_2O$) from the melt by evaporation of component i (for instance NaOH) diffusing through a gas boundary layer above the melt is given by Beerkens [38]:

$$Q_j = (n/q) \cdot Sh_{g,i} \cdot (D_{g,i}/y) \cdot (p_i^* - p_{b,i})/(R \cdot T) \,. \tag{9}$$

In most glass furnace combustion spaces, the gas flows (velocity $v_g$) are mainly turbulent or disturbed. The distance from the leading edge (position where the gas flow first touches the glass melt surface) is given by the value $y$ (in m). The vapor pressure of component i in the bulk gas flow is $p_{b,i}$.

The Sherwood number ($Sh_g$) expression for turbulent gas flows along a length $L_g$ (length from the leading edge of the gas flow touching/streaming above the glass melt surface) leads to the equation for the average loss ($\bar{Q}_j$ in mol/(m$^2$ · s)) of component j over this length $L_g$ [38]:

$$\bar{Q}_j = (n/q) \cdot A \cdot v_g^{0.8} \cdot \varrho_g^{0.47} \cdot \mu_g^{-0.47} \cdot D_{g,i}^{0.667} \cdot L_g^{-0.2} \cdot R^{-1} \cdot T^{-1} \cdot (p_i^* - p_{b,i}) \,. \tag{10}$$

The properties $\sigma_g$, $\mu_g$, $D_{g,i}$ are respectively the average gas density, gas viscosity and diffusion coefficient in the gas phase in the boundary layer above the melt. $R$ is the gas constant.

The dimensionless factor $A$ is in the range of 0.03 to 0.04. For $p_{b,i} \ll p_i^*$ the term $p_{b,i}$ can be neglected and in a certain composition range, the vapor pressure of component i can be assumed to be proportional to the local surface concentration (at $x = 0$) of component j in the melt: $p_i^* = B \cdot C_{j,x=0}(t)$. These two assumptions allow the analytical solution of the differential equation (4) with boundary conditions given by equations (5) and (10) and neglecting of $p_{b,i}$.

For a static melt exposed to a flowing gas atmosphere the value of $C_j$ depends on time, since depletion by the evaporation process is not completely compensated by the limited diffusion rates in the glass melt. The proportionality factor $B$ depends on temperature, glass composition and the concentration of the reacting gas k, but due to a nonlinear relation of the vapor pressure $p_i$ and concentration $C_j$ in a wider composition range, this proportionality factor can only be used as an estimate for a limited composition range.

The term

$$\bar{Q}_i = (n/q) \cdot A \cdot v_g^{0.8} \cdot \varrho_g^{0.47} \cdot \mu_g^{-0.47} \cdot D_{g,i}^{0.667} \cdot L_g^{-0.2} \cdot R^{-1} \cdot T^{-1} \cdot B \cdot C_{j,x=0}(t) \tag{11}$$

can be calculated for known values of $C_{j,x=0}(t)$. For well-mixed melts, this value is equal to the bulk concentration of component j in the melt. However, for static melts or almost static melts exposed during a certain time period this value will decrease due to depletion.

The average depletion and average time dependent loss of component j from such a melt exposed to a flowing gas with velocity $v_g$ along a surface with length $L_g$ can analytically be calculated by the application of equation (12) and (13) derived from [39] and given below. For the total loss of component j ($M_{m,j}$ in mol/m$^2$) from the melt during exposure time $t$ by integration of $\bar{Q}_i$ over this time, the expression

$$M_{m,j} = (C_{j,0}/H_d) \cdot \{\exp(H_d^2 \cdot D_{m,j} \cdot t) \cdot \operatorname{erfc}[H_d \cdot (D_{m,j} \cdot t)^{0.5}] - 1 + 2H_d \cdot (D_{m,j} \cdot t/\pi)^{0.5}\} \tag{12}$$

and for the surface concentration the relation

$$C_{j,x=0}(t) = C_{j,0} \cdot \exp(H_d^2 \cdot D_{m,j} \cdot t) \cdot \operatorname{erfc}[H_d \cdot (D_{m,j} \cdot t)^{0.5}] \tag{13}$$

can be applied and where $H_d$ is defined as:

$$(n/q) \cdot A \cdot v_g^{0.8} \cdot \varrho_g^{0.47} \cdot \mu_g^{-0.47} \cdot D_{g,i}^{0.667} \cdot L_g^{-0.2} \cdot R^{-1} \cdot T^{-1} \cdot B/D_{m,j} \,.$$

$H_d$ is an expression (dimension m$^{-1}$), relating the mass transfer coefficient for the evaporating species in the gas phase to the diffusion coefficient of the volatile component in the melt. $C_{j,0}$ is the initial concentration and bulk concentration of component j in the melt. Differentiation of equation (12) to time gives the mass loss rate of component j (due to reaction (7)) from a melt exposed to flowing gas atmosphere after exposure time $t$, averaged over the surface length $L_g$ (length of melt in direction of the gas flow).

## 6. Sodium evaporation kinetics from soda–lime–silica glass melts

The evaporation process of sodium compounds from container, tableware and float glass melts is of great technological importance. This process determines the dust formation, fouling of regenerators and chemical attack of refractory materials in the superstructure in a large number of glass furnaces. An example is the evaporation loss of $Na_2O$ by NaOH formation. For a float glass composition the vapor pressure (in Pa) of NaOH can be estimated by

$$p^*_{NaOH} = 210 \cdot p^{0.5}_{H2O} \cdot C_{Na2O,x=0}(t) \cdot \exp(-25617/T) \quad (14)$$

where $p_{H2O}$ is given in Pa, $C_{Na2O,x=0}(t)$ is the surface concentration of $Na_2O$ in the melt given in mol/m$^3$ and $T$ is surface temperature given in K. As said before, the value of $C_{Na2O,x=0}(t)$ will decrease as exposure time ($t$) at the glass melt surface increases due to $Na_2O$ depletion. In this case the value of $B_{NaOH}$ is $210 \cdot p^{0.5}_{H2O} \cdot \exp(-25617/T)$ for compositions close to compositions of common float glasses.

Sodium may evaporate by reaction with water, forming NaOH or by reduction due to reactions with CO or with not completely burnt hydrocarbon components in the combustion space. In that case the loss of $Na_2O$ can be given by:

$$Q_{Na2O} = 1/2 \cdot A \cdot v_g^{0.8} \cdot \varrho_g^{0.47} \cdot \mu_g^{-0.47} \cdot D^{0.667}_{g,NaOH} \cdot L_g^{-0.2} \cdot R^{-1} \cdot T^{-1} \cdot B_{NaOH} \cdot C_{Na2O,x=0}(t) + 1/2 \cdot A \cdot v_g^{0.8} \cdot \varrho_g^{0.47} \cdot \mu_g^{-0.47} \cdot D^{0.667}_{g,Na} \cdot L_g^{-0.2} \cdot R^{-1} \cdot T^{-1} \cdot B_{Na} \cdot C_{Na2O,x=0}(t) . \quad (15)$$

$B_{Na}$ is the proportionality factor between the $Na_2O$ concentration at the glass melt surface and the sodium vapor pressure; this factor depends on the CO pressure just above the melt and temperature. $H_d$ is now defined as:

$$H_d = 1/2 \cdot A \cdot v_g^{0.8} \cdot \varrho_g^{0.47} \cdot \mu_g^{-0.47} \cdot D^{0.667}_{g,NaOH} \cdot L_g^{-0.2} \cdot R^{-1} \cdot T^{-1} \cdot B_{NaOH}/D_{m,Na2O} + 1/2 \cdot A \cdot v_g^{0.8} \cdot \varrho_g^{0.47} \cdot \mu_g^{-0.47} \cdot D^{0.667}_{g,Na} \cdot L_g^{-0.2} \cdot R^{-1} \cdot T^{-1} \cdot B_{Na}/D_{m,Na2O} . \quad (16)$$

Equations (15) and (16) can be extended for more $Na_2O$ evaporation reactions, forming for instance: NaO, $Na_2SO_4$, NaCl vapors. The evaporation loss of $Na_2O$ and depletion of $Na_2O$ at the glass surface can be determined by the substitution of this $H_d$ value in equations (12) and (13).

## 7. Modeling results for sodium evaporation processes

The previously described kinetic model has been applied to predict the sodium evaporation losses from soda–lime–silica melts under industrial conditions or for laboratory scale experiments. Sanders and Schaeffer [10] pointed out that depletion of sodium at the surface of a soda–lime glass melt exposed to a humid gas atmosphere at 1335 °C hardly can go down to $Na_2O$ concentration levels below 11.5 wt% even at very long exposure times. A thermodynamically stable surface composition seems to be established at these relatively low temperatures. However, for much higher temperatures, above 1450 °C, such a stabilization of the glass melt surface composition is not expected. Depletion of $Na_2O$ concentrations at the surface of common soda–lime glass melts below 11 wt% may be expected for very high temperatures and high NaOH evaporation rates. However, $Na_2O$ depletion from 13 % down to values below 10 % is not expected under normal industrial conditions.

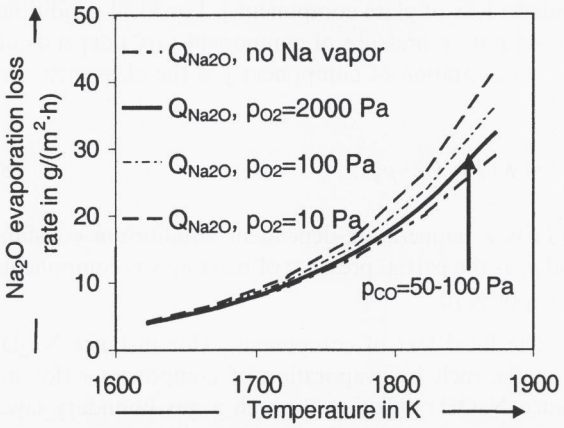


Figure 2. Effect of temperature and oxidation state of furnace atmosphere on sodium oxide evaporation loss from stirred soda–lime–silica float glass melt (no depletion at surface), exposed to humid gas atmosphere with $0.18 \cdot 10^5$ Pa water vapor pressure and a gas velocity of 10 m/s.

Figure 2 shows the effect of temperature on the modeled evaporation loss rates of $Na_2O$ from a float glass melt, due to NaOH and sodium formation at the glass melt surface. Sodium (Na) formation becomes important for $p_{O2} < 100$ to 500 Pa.

Typically, glass melt volumes are exposed to the surface during 10 to more than 300 min in industrial glass furnaces. In case that the top layer of the melt (a few mm thickness) can be considered to be static, depletion of volatile species will take place. A concentration profile of the evaporating glass component extends over 0.3 to 3 mm in the melt, depending on the diffusion coefficient and exposure time.

Figure 3a shows the decreasing evaporation loss rate of $Na_2O$ (evaporating as NaOH and Na), due to depletion of the $Na_2O$ concentration at the glass melt surface at increasing exposure times and in the case of no mixing or no convection effects in the surface glass layer. At high temperatures, depletion becomes more pronounced and the surface concentration of $Na_2O$ will decrease considerably and evaporation reduces as exposure time proceeds. Figure 3b shows the decrease in $Na_2O$ surface concentration during this evaporation process (after 2 h exposure).

The evaporated sodium species in most soda–lime–silica furnaces will mainly form sodium sulfate dust during the cooling process of the flue gases as shown by

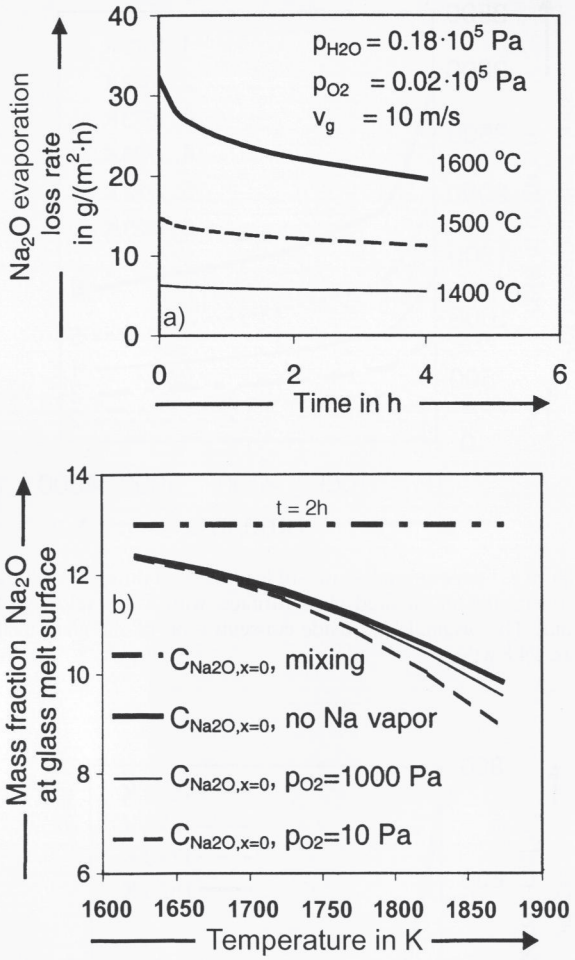


Figures 3a and b. Evaporation from float glass melt surface exposed to combustion gases with a velocity of 10 m/s and water vapor pressure of $0.18 \cdot 10^5$ Pa; a) calculated sodium evaporation loss rate from static melt, b) calculated sodium oxide concentration, $C_{Na2O,x=0}(t)$, at surface of well-mixed and static float glass melt after 2 h.

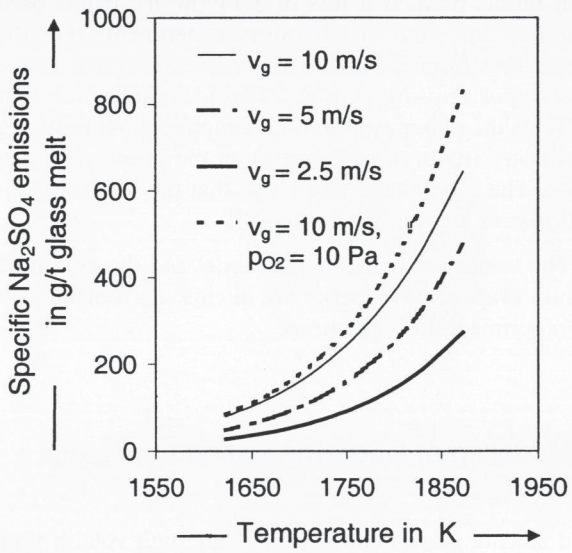


Figure 4. Sodium sulfate dust emissions as a function of temperature and gas velocity above soda–lime–silica glass melt in air–natural gas fired glass furnaces with moderate oxygen excess ($p_{O2}$ = 100 Pa).

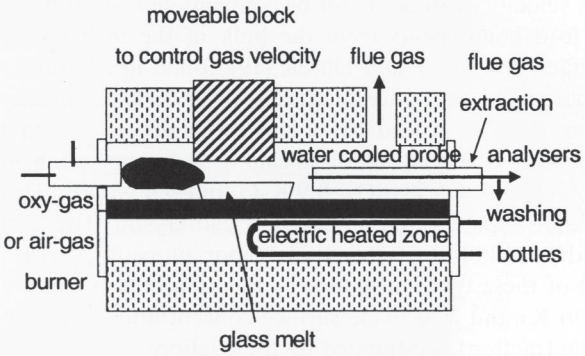


Figure 5. Laboratory equipment for experimental investigation of evaporation processes from glass melts exposed to combustion gases.

reaction equilibria equations (2) and (3). Figure 4 shows the effect of temperature and gas velocity above the melt on the calculated sodium sulfate particulate emissions for a typical soda–lime–silica glass furnace, due to sodium evaporation processes. Note the increased dust emission levels for very low oxygen concentrations in the combustion space. At these low oxygen levels ($p_{O2} \ll 100$ Pa) reduction at the glass melt surface stimulates sodium (Na) evaporation.

## 8. Evaporation experiments

Figure 5 schematically shows the laboratory equipment applied in this study to measure evaporation losses from glass melts exposed to combustion atmospheres generated by air or oxygen firing. This equipment allows the determination of the volatilization of different glass melt components at adjusted temperatures and gas velocity levels. An aluminum oxide sample boat with glass melt surface dimensions of 6 by 15 cm is used for containing the melt. The evaporation rates, as measured for most volatile glass components exposed to the flames, indeed depend on the gas velocity and are proportional to $v_g^{0.8}$. This dependency may disappear when diffusion in the glass melt becomes the determining step for the evaporation rate.

As an example, the sodium component evaporation rates at an average glass melt surface temperature of 1380 to 1390 °C and exposed to the combustion gases of an oxygen–natural gas burner with 55 vol.% water vapor and a bulk gas velocity of 1 m/s have been measured. At oxidizing conditions the evaporation loss rate of $Na_2O$ is determined on 3.5 to 4 g/(m² h). The evapor-

ation model predicts a loss of 3.4 g/(m$^2$ h). It has been shown by this kind of laboratory experiments that the sodium loss from the melt is indeed proportional to the water vapor pressure: $\sim p_{H2O}^{0.5}$. This is an indication that NaOH is the major evaporating component. At reducing conditions (natural gas excess) evaporation rates increase. The experiments show also that the sodium evaporation rate is proportional to $v_g^{0.8}$.

The trends predicted by the model and the estimated sodium evaporation kinetics are in close agreement with the experimental observations.

## 9. Modeling of lead evaporation from glass melts

Lead silicate glasses show a relatively high volatility of lead components during melting. The high evaporation loss often leads to formation of a glass melt top layer depleted in lead oxide. This phenomenon has already been observed by Kruithof, La Grouw and de Groot [6] and often results in glass products with cord.

The strong evaporation loss at high temperatures and gas velocities can often not be compensated by diffusion of lead components from the bulk of the melt to the surface. Matoušek and Hlavac [19], found in laboratory experiments at moderate gas flows at 1300 °C already more than 50 % lead oxide surface depletion after 8 h exposure of a lead alkali silicate melt (composition in wt%: 24.8 PbO, 58 $SiO_2$, 9.9 $K_2O$ and 4.4 $Na_2O$). This type of glass is often applied for lead crystal. The lead oxide equilibrium (saturation) vapor pressure $p^*_{PbO}$ (in Pa) of these types of glasses as function of temperature ($T$ in K) and lead oxide surface concentration ($C_{PbO}$ in mole fraction) is estimated by the relation:

$$p^*_{PbO} = C_{PbO} \cdot 2.06 \cdot 10^{11} \cdot \exp(-27520/T) \,. \qquad (17)$$

Evaporation models for lead oxide can be derived similar to the model applied for predicting NaOH or Na evaporation.

Both the mass transfer of lead vapors in the gas phase, through the boundary layer and diffusion mass transfer processes in the glass melt determine the lead evaporation kinetics. Figure 6 shows the evaporation loss rate as a function of time, at different temperatures during melting of lead silicate glass in an air–natural gas fired furnace. Figure 7 shows the progress of the depletion of lead oxide in the static surface layer during this evaporation process, calculated by the model. In the figure is shown that depletion of the lead oxide at the surface hardly depends on temperature. At higher temperatures lead oxide evaporation losses will be enhanced, but diffusion of lead oxide in the melt becomes also faster at increasing temperatures, compensating for the evaporations loss at the surface. At reducing firing conditions lead oxide reacts at the glass surface with CO

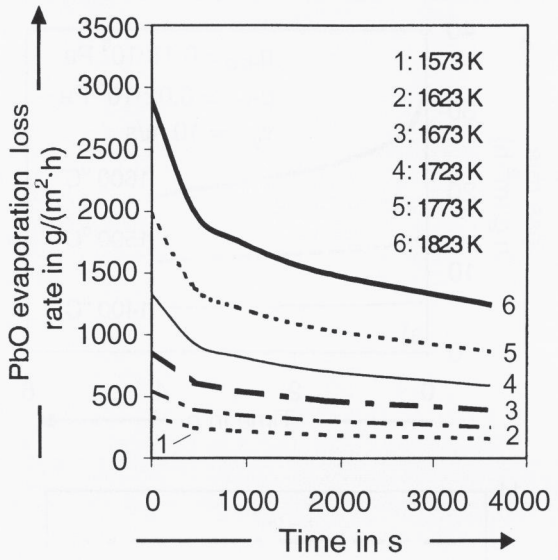


Figure 6. Evaporation loss rate of lead oxide at different melting temperatures in air-fired glass furnace, with a gas velocity of 8 m/s. The original lead oxide concentration of the glass melt was: 24.8 wt%.

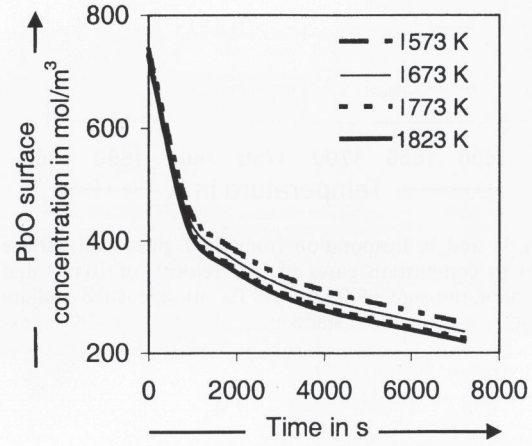


Figure 7. Depletion of lead oxide at the lead silicate glass melt surface, during evaporation process in glass furnace.

or with not completely burnt hydrocarbon compounds forming lead vapor. Reducing conditions will strongly stimulate lead losses from lead silicate melts. This observation has also been confirmed for lead evaporation from container glass melts, using cullet contaminated with lead glass. Reducing gas atmospheres or lower redox states (more reduced glass) enhance lead evaporation in container glass furnaces.

## 10. Modeling of gas velocity in combustion space of glass furnaces

CFD models for simulation of the processes in the combustion spaces of glass furnaces [40 and 41] can be ap-

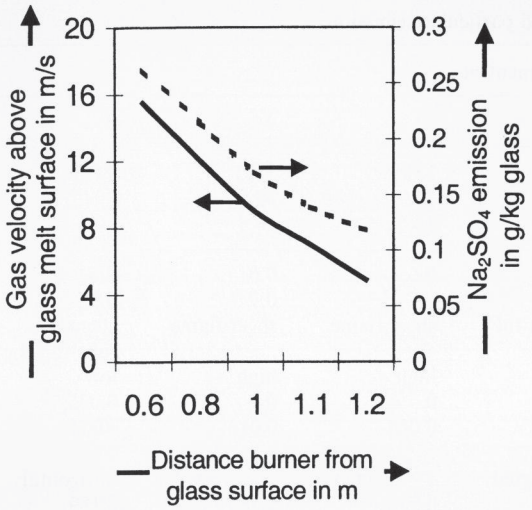


Figure 8. Calculated gas velocity above glass melt and specific dust emissions (calculated by combustion and evaporation models), depending on distance between burner and glass surface in a typical end-port fired glass furnace.

plied to calculate or estimate the gas flows above the glass melt as a function of the distance from the burner. An increase of the distance between the glass melt surface and the horizontally arranged burners will lead to a decrease of the gas velocity just above the melt.

Figure 8 shows the calculated gas velocity just above the melt for an end-port fired glass furnace as a function of the distance between the plane in which the burners are placed and the glass surface. The effect of the gas velocity on the evaporation rate of NaOH can be predicted by the evaporation model. In the same figure the specific sodium sulfate dust emission is shown as a function of the burner–glass melt distance assuming that all evaporated NaOH will be converted in sodium sulfate dust during the cooling of the flue gases. This figure shows the importance of the burner position on evaporation and emissions for the typical situation of an industrial soda–lime glass furnace. Convection of heat from the combustion space to the glass melt surface has a minor effect on the overall effective heat transfer in glass furnaces, since radiation of heat from the flames and crown are predominant in transferring the combustion heat to the melt. Thus, it is recommended to avoid a short distance between burners and glass melt surface in order to lower or limit evaporation rates of glass components, which then probably will lead to less refractory attack or emissions.

## 11. Emission reduction in industrial glass furnaces

Modeling results for the conditions of industrial furnaces show that a combination of measures: increasing burner–glass melt distance and avoiding excessive glass melt temperatures will be very effective in the reduction of emissions. Table 2 demonstrates this for two cases.

Table 2. Estimated sodium concentrations and dust emissions for industrial soda–lime glass furnaces, depending on process conditions

| process conditions | furnace 1 | furnace 2 |
|---|---|---|
| average surface temperature in °C | 1500 | 1450 |
| glass type | float glass | float glass |
| NaCl in soda in wt% | 0.25 | 0.15 |
| gas velocity above melt in m/s | 10 | 5 |
| oxygen pressure above melt in Pa | 10 | 1000 |
| energy consumption in GJ/t glass | 5.5 | 5.5 |
| NaOH in atmosphere in Pa | 7.5 | 3.0 |
| $Na_2SO_4$ dust emissions in mg/m$^3$ | 200 to 250 | 90 to 100 |

NaCl present as contaminant in synthetic soda types often evaporates easily during the melting of the batch and finally forms HCl gas and sodium sulfate dust. A reduction from 0.25 wt% NaCl in the soda down to 0.15 % in a float glass furnace with 25 % cullet leads to a decrease of about 30 mg sodium sulfate dust per m$^3$ flue gas (273.15 K, 101.3 kPa, 8 % oxygen, dry).

Flames touching the glass melt surface will consequently lead to high CO concentration levels and low $p_{O2}$ values just above this surface, enhance the evaporation of alkali and lead compounds. An increase of the distance burner–glass melt from 0.6 to 0.7 m to more than 1 m lowers the gas velocities by about 50 % and lowers the risk of reduction of glass melt components.

The situations in table 2 show the potential of primary measures to reduce alkali vapor attack, which depends strongly on the NaOH vapor pressure in the furnace atmosphere [2] and the possibility to lower dust emissions.

## 12. Industrial tests and measurements

The described models for the evaporation process of sodium or lead can be extended for other components such as potassium, antimony or boron species and other glasses, but the chemical activity of these compounds in the glass melt or the vapor pressures as function of glass composition should be known and the glass melt diffusion coefficients of these volatile glass components have to be determined or have to be predicted [42]. In this study, only modeling of sodium evaporation has been carried out to demonstrate the validity and application of such evaporation models to understand emissions and evaporation processes in industrial furnaces. In the previous sections it has been shown that glass melt temperature, gas velocity and composition of glass

Table 3. Operational conditions of soda–lime glass furnaces and measured particulate emissions

| | furnace burner arrangement no. | | | | |
|---|---|---|---|---|---|
| | 1 | 2 | 3 | 4 | 5 |
| average glass melt surface temperature in °C | 1494 | 1494 | 1511 | 1511 | 1453 |
| surface area in $m^2$ | 39 | 39 | 39 | 39 | 60 |
| $Na_2O$ content of glass in wt% | 16.5 | 16.5 | 16.5 | 16.5 | 16.5 |
| water vapor pressure in furnace atmosphere in $10^5$ Pa | 0.6 | 0.6 | 0.6 | 0.6 | 0.6 |
| glas velocity above melt in m/s | 0.5 | 0.5 | 0.7 | 0.7 | 0.7 |
| burner type | tube-in-tube | tube-in-tube | sheet flame | sheet flame | staged, tube-in-tube |
| low momentum/high momentum | high | high | high | high | low |
| oxygen pressure above melt in $10^5$ Pa | 0.03 | 0 | 0 | 0 | 0.005 |
| CO-pressure above melt in $10^5$ Pa | 0.001 | 0.065 | 0.065 | 0.013 | <0.001 |
| burner horizontal or directed to glass melt surface | horizontal | 7° directed | 7° directed | 7° directed | horizontal |
| dust emission in kg/t glass | 0.276 | 0.398 | 0.559 | 0.485 | 0.189 |
| $Na_2O$ emission in kg/t glass | 0.096 | 0.190 | 0.315 | 0.262 | 0.087 |
| NaOH concentration in furnace atmosphere in Pa | 21.8 | 26.0 | 36.0 | 38.5 | 9.9 |

melt and furnace atmosphere are key parameters in the kinetics of evaporation of alkali and lead. For a few oxygen-fired soda–lime–silica glass furnaces, modeling of sodium evaporation has been carried out. Modeling for these different but similar furnaces, all producing the same type of glass, but for different burner settings, has been performed. Table 3 shows some process data of these furnaces. Although, the furnaces are of the same design type and the same glass composition and raw materials are similar, the specific dust and sodium emissions are distinctly different. As the evaporation model results show, the burner settings and the reducing/oxidizing combustion conditions greatly effect the evaporation of sodium species. Figure 9 shows the results of the industrial measurements: obviously changes in the position and type of burner and the oxygen–natural gas ratio (determining $p_{O2}$ and $p_{CO}$ vapor pressures) will cause large differences in dust emissions and sodium evaporation. The gas velocities and glass melt surface temperatures in these furnaces are calculated with a CFD model [41]. The model results for NaOH evaporation and $Na_2O$ losses show the same trend as the measurements. The evaporation loss of $Na_2O$ from 30 % of the surface area with the highest temperatures (hot spot) has been calculated for these furnaces. According to the values in figure 9, about 60 to 80 % of the sodium evaporates from this area.

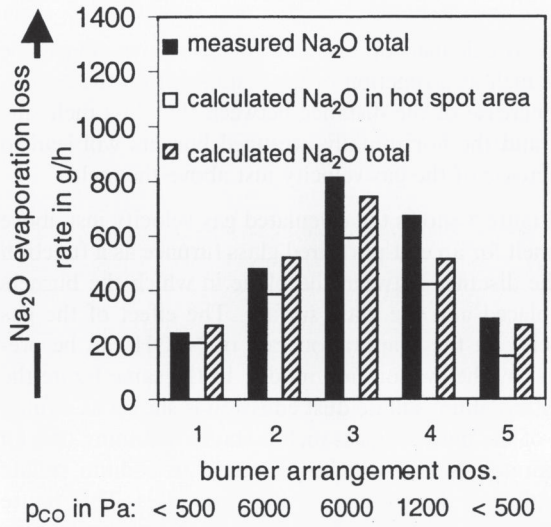


Figure 9. Measured sodium evaporation rates and calculated average $Na_2O$ emissions for industrial natural gas–oxygen fired soda–lime glass furnaces. The CO vapor pressure (in Pa) measured just above the melt is indicated and the evaporation from the hottest zone (30 % of glass surface) is also given in the graph. Bar 1 = tube-in-tube burner horizontal, oxidizing conditions; bar 2 = tube in tube burner, reducing flames; bar 3 = burner for sheet (flat) flame directed to glass surface, reducing flames; bar 4 = burner for sheet (flat) flame directed to glass surface, mild-reducing flames; bar 5 = tube-in-tube burner staged combustion, horizontal.

Evaporation modeling and tests have also been performed to compare the evaporation process in an oxygen– and air–gas-fired furnace both melting the same amber glass type. Taking the changed combustion atmosphere into account: about 18 vol.% water vapor versus 56 vol.% for respectively the air and oxygen fired furnace and the lower gas velocities in the oxygen–gas-fired melter, a decrease of the specific $Na_2O$ emissions ($Na_2O$ in the dust) of about 45 % is expected by the evaporation model, the measurement showing a decrease of 28 %. The evaporation model applied for these two furnaces uses roughly estimated data for the average glass surface temperature and gas velocity and this partly explains the difference between measurement and model result.

## 13. Evaporation of other species from glass melts

Boron evaporation from borosilicate melts, potassium loss and antimony volatilization from TV glass melts or from alkali lead silicate melts are also important phenomena in the glass industry. In all cases, an increase in glass-melt surface temperature and gas velocity will enhance evaporation losses from alkali–earth alkali silicate, borosilicate, lead glass and TV glass melts. Reducing conditions, for instance reducing parts of flames will promote the evaporation of lead and alkali from these glass melts, due to reduction of the oxides at the glass melt surface. Water vapor may react to form components such as, NaOH, KOH, $Pb(OH)_2$, $HBO_2$ or $Sb(OH)_3$. The evaporation of potassium also depends on the water vapor pressure, similar to the evaporation of sodium by formation of hydroxide species.

However, for alkali borosilicate melts, the major evaporating species expected from such melts are $NaBO_2$ and $KBO_2$, the NaOH, $HBO_2$ and KOH vapor pressures are much lower than the alkali meta-borate pressures above the melt. Thus, the water vapor pressure in the combustion space above the melt is not strongly decisive for the boron and alkali losses of such melts. The higher water vapor concentration in oxygen-fired furnaces compared to air-fired furnaces will hardly increase the total vapor pressure of boron species or alkali species for alkali borosilicate glasses such as being used for insulation glass wool. In oxygen-fired furnaces, producing less volume of combustion gases, the gas velocity above the melt can be kept relatively low compared to air-fired furnaces. This will offer the possibility to reduce the evaporation from these alkali borosilicate glasses when melting in oxygen-fired furnaces. For low alkali borosilicate melts, such as for an E-glass melt, an increasing water vapor level will enhance $HBO_2$ evaporation, one of the main evaporating components in E-glass.

The high evaporation rates for borosilicate and lead glasses often lead to a glass melt top layer typically at a thickness of 0.5 to 3 mm depleted in boron, alkali (boron boosts the evaporation of alkali by formation of volatile alkali meta-borates) and /or lead. This may cause the formation of cord.

The main vapor components, originating from TV panel glass melts or batch, present in the furnace atmosphere are: KOH, NaOH, $Sb(OH)_3$, NaCl (when using chloride-containing soda).

From C-glass melts (sodium borosilicate melts) the vapors are mainly: $NaBO_2$, NaOH, NaCl, $KBO_2$. From E-glass melts, vapors from the glass include: $HBO_2$, $KBO_2$ and a small amount of $NaBO_2$. High temperatures and gas velocities above E-glass melts will lead to strong depletion of boron and alkali at the top surface of the melt, especially >1550 °C. Laboratory experiments have shown that at high temperatures and at high gas velocities, the evaporation of boron and alkali from the molten glass becomes hardly dependent on the composition of the gas phase and almost independent on gas velocity. The evaporation rate is predominantly governed by the diffusion processes in a melt, due to formation of a static layer at the top very much depleted in these volatile species (boron concentrations can drop more than 50 %).

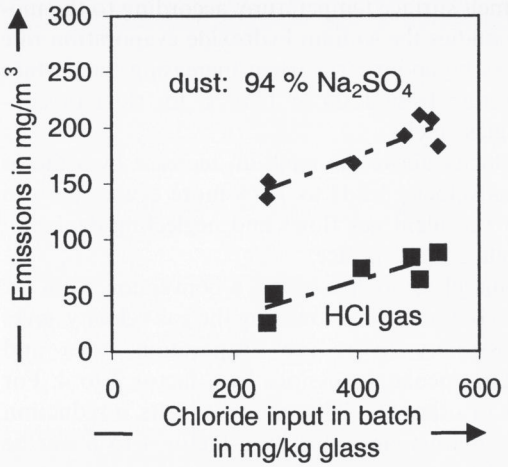


Figure 10. HCl and dust emissions, measured before filter and scrubber system, during tests with different soda qualities in a float glass furnace.

During the cooling of the exhaust gases, condensation reactions start below 1050 to 1150 °C and salts are formed, in presence of $SO_2$ gas: $Na_2SO_4$, $K_2SO_4$ and $PbSO_4$ can be formed.

Figure 10 shows the effect of the total NaCl input in a float glass furnace [37] and measured dust (mainly sodium sulfate) and HCl emissions in the raw flue gases (before a filtering unit). The first 0.200 g NaCl present in the batch per ton glass are absorbed almost completely in the soda–lime–silica glass. About 50 % of the extra NaCl added to the batch evaporates and forms HCl and sodium sulfate dust. The dust itself hardly contains NaCl.

## 14. Conclusions and recommendations

The evaporation model and laboratory results show the most important key process parameters which govern the evaporation kinetics of glass melt components such as alkali, lead, boron, chlorides or antimony. These parameters are:

- Glass melt composition, a high chemical activity of a glass melt component often increases the vapor pressure, the activity depends strongly on the glass compositions.

- Glass melt surface temperature: according to the modeling studies the sodium hydroxide evaporation rate increases by about 50 % when increasing the surface temperature from 1500 to 1550 °C for float or container glass melts.
- Gas velocity above the melt: an increase by a factor 2 in gas velocity leads to 75 % more evaporation in case of turbulent gas flows and neglecting depletion at the glass melt surface.
- For some glass compositions, a conversion from air firing to oxygen firing, lowering the gas velocity, gives the possibility to reduce evaporation rates and specific particulate emissions by a factor 2 to 4. For C-glass or other alkali borosilicate melts, a reduction of specific dust emissions by a factor 4 to 5 can be achieved.
- An increasing distance between horizontally positioned burners and the glass melt surface lowers the mass transfer rate in the gas phase and often decreases evaporation rates.
- Strongly reducing conditions ($p_{O2}$ < 100 Pa) at the glass melt surface may increase evaporation of alkali and lead by 20 to 40 %.
- The NaOH vapor pressure for a soda–lime glass with 16 wt% $Na_2O$ is estimated to be about 20 to 25 % higher than for a composition with 13 % $Na_2O$.
- Contamination of glass-forming raw material batch or cullet by lead or chlorides will often increase evaporation. An increase of 300 g chloride (495 g NaCl) up to 450 g Cl in the batch, per ton glass, leads to about 100 g extra dust emissions per ton glass.

Industrial tests show the potential for reduction of dust emissions by primary measures. Oxygen firing may be an important method for the reduction of specific dust emission from lead and alkali borosilicate glass furnaces, since lower gas velocities will decrease the mass transfer rates and water vapor has a minor effect on evaporation losses from especially alkali borosilicate melts. Burner selection, burner re-positioning and burner control and avoiding NaCl contamination in the raw materials show to be effective ways to reduce sodium evaporation and dust emissions and it may lower the potential for refractory superstructure corrosion by alkali vapors.

## 15. References


[1] Kircher, U.: Fortschritte bei der Abgasreinigung von Glasschmelzöfen. Glastech. Ber. **59** (1986) no. 12, p. 333–343.

[2] Faber, A. J.; Beerkens, R. G. C.: Reduction of refractory corrosion in oxy-fuel glass furnaces. In: Proc. XVIII International Congress on Glass, San Francisco, CA, 1998. Westerville, OH: Am. Ceram Soc., 1998. Session A09. (Available on CD-ROM.)

[3] Gebhardt, F.: Emissionen von Glasschmelzwannen und deren Minderung durch schmelztechnische Maßnahmen. Glastech. Ber. **59** (1986) no. 12, p. 344–349.

[4] Beerkens, R. G. C.; De Waal, H.: Simulation of the condensation and deposition processes in regenerators of glass furnaces. Glastech. Ber. **61** (1988) no. 2, p. 36–42.

[5] Mutsaers, P. L. M.; Beerkens, R. G. C.; De Waal, H.: Fouling of heat exchanger surfaces by dust particles from the flue gases of glass furnaces. Glastech. Ber. **62** (1989) no. 8, p. 266–273.

[6] Kruithof, A. M.; La Grouw, C. M.; De Groot, J.: Volatilization of glass. In: Proc. Symposium sur la fusion du verre, Bruxelles 1958. Charleroi: Union Scientifique Continentale du Verre, 1958. p. 515–527.

[7] Dietzel, A.; Merker, L.: Entstehung von Inhomogenitäten in der Glasschmelze durch Verdampfung einzelner Glasbestandteile. I. Glastech. Ber. **30** (1957) no. 4, p. 134–138.

[8] Ehrig, R.: Zum Problem der Oberflächenverdampfung aus Alkaliborosilikatglasschmelzen. Silikattechnik **24** (1973) nos. 8–9, p. 296–298.

[9] Stockham, J. D.: The composition of glass furnace emissions. J. Air Poll. Ass. **21** (1971) no. 11, p. 713–715.

[10] Sanders, D. M.; Schaeffer, H. A.: Reactive vaporization of soda-lime-silica glass melts. J. Am. Ceram. Soc. **59** (1976) nos. 3–4, p. 96–101.

[11] Sanders, D. M.; Haller, W. K.: Effect of water vapor on sodium vaporization from two silica-based glasses. J. Am. Ceram. Soc. **60** (1977) nos. 3–4, p. 138–141.

[12] Hanke, K. P.; Scholze, H.: Einfluß der Ofenatmosphäre auf die Verdampfung aus Glasschmelzen. Glastech. Ber. **50** (1977) no. 11, p. 271–275.

[13] Sanders, D. M.; Wilke, M. E.; Hurwitz, S. et al.: Role of water vapor and sulfur compounds in sodium vaporization during glass melting. J. Am. Ceram. Soc. **64** (1981) no. 7, p. 399–404.

[14] Conradt, R.; Scholze, H.: Zur Verdampfung aus Glasschmelzen. Glastech. Ber. **59** (1986) no. 2, p. 34–52.

[15] Cable, M.; Fernandes, M. H.: Volatilization of molten sodium metaborate with convection of the furnace atmosphere. Phys. Chem. Glasses **39** (1998) no. 4, p. 228–235.

[16] Barlow, D. F.: Volatilisation of fluorides, borates and arsenic from glass. In: Proc. VIIe Congress International du Verre, Bruxelles 1965. Vol. I.I.2. p. 1–14.

[17] Wenzel, J. T.; Sanders, D. M.: Sodium and boron vaporization from boric oxide and borosilicate glass melt. Phys. Chem. Glasses **23** (1982) no. 2, p. 47–52.

[18] Schaeffer, H. A.; Sanders, D. M.: Verdampfungsvorgänge an einem $Na_2O$-CaO-$SiO_2$-Glas, Dampfdruck- und Konzentrationsprofilmessungen. Glastechn. Ber. **49** (1976) no. 5, p. 95–102.

[19] Matoušek, J.; Hlavac, J.: A study of the volatilisation of lead glass. Glass Technol. **12** (1971) no. 4, 103–106.

[20] Terai, R.; Ueno, T.: Volatilization of components from glasses containing high lead oxide at high temperature. J. Ceram. Assoc. Jpn. **74** (1966) p. 283–295.

[21] Cable, M.; Apak, C.; Chaudhry, M. A.: The kinetics of volatilization from lead glasses. Glastechn. Ber. **48** (1975) no. 1, p. 1–11.

[22] Cable, M.; Chaudhry, M. A.: Volatilisation from soda-lime-silica melts at one atmosphere and reduced pressures. Glass Technol. **16** (1975) no. 6, p. 125–134.

[23] Murai, S.; Wenzel, J.; Sanders, D. M.: Vaporisation in an unstirred soda-lime-silica glass melt. Phys. Chem. Glasses **21** (1980) no. 4, p. 150–155.

[24] Oldfield, L. F.; Wright, R. D.: The volatilization of constituents from borosilicate glass at elevated temperatures. In: Advances in Glass Technology. Proc. VI Int. Congress on Glass, Washington, DC, 1962. New York: Plenum, 1962. p. 35–51.

[25] Hrma, P.: Effects of surface forces in glass technology (a review). Glass Technol. **23** (1982) no. 3, p. 151–155.

[26] Bonnel, D. W.; Hastie, J. W.: Transpiration mass spectrometry of high temperature vapors. NBS Spec. Publ. **561** (1979). In: Proc. 10th Materials Research Symposium on

Characterization of High Temperature Vapors and Gases 1979. p. 357–409.
[27] Drowart, J.; Colin, R.; Exsteen, G.: Mass-spectrometric study of the vaporization of lead-monoxide. Trans. Faraday Soc. **61** (1965) p. 1376–1383.
[28] Gorokhov, L. N.; Gusarov, A. V.; Makarov, A. V. et al.: Mass spectrometric study of the evaporation of alkali metaborates. High Temp. Sci. **9** (1971) p. 1082–1085.
[29] Matoušek, J.; Piacente, V.; Ferro, D. et al: Alkali evaporation from multicomponent lead glasses. Glass Technol. **19** (1978) no. 6, p. 158–161.
[30] Heide, K.; Harting, E.; Schmldt, H. G. et al.: Untersuchungen zur Verdampfung von Bor beim Einschmelzen von borhaltigen Glasgemengen. Glastech. Ber. **59** (1986) no. 3, p. 59–63.
[31] Kassis, N.; Frischat, G. H.: Dampfdrücke von Glasschmelzen des Mischalkalisystems $Na_2O$-$Rb_2O$-$SiO_2$. Glastechn. Ber. **54** (1981) no. 4, p. 89–98.
[32] Bale, C. W.; Pelton, A. D.: FACT-Win-User Manual. CRCT, Ecole Polytechnique de Montréal, Québec, Canada, Jan. 1999. (Available on the Internet: http://www.crct.polymtl.ca.)
[33] Pelton, A. D.; Eriksson, G.: A thermodynamic database computing system for multicomponent glasses. In: Bickford, D. F. et al. (eds.): Advances in the Fusion of Glass. Proc. 1st Int. Conf. on Advances in the Fusion of Glass, Alfred, NY 1988. Westerville, OH: Am. Ceram. Soc., 1988, p. 27.1–27.11.
[34] Hoheisel, H. P.; Schaeffer, H. A.: Einfluß der Bleiverdampfung auf die chemische Resistenz von PbO-$SiO_2$ Gläsern. Glastechn. Ber. **50** (1977) no. 11, p. 286–295.
[35] Scholze, H.; Tünker, G.; Conradt, R.: Verdampfung von Fluor aus Glasschmelzen und beim Einschmelzprozeß. Glastechn. Ber. **56** (1983) nos. 6–7, p. 131–137.
[36] Carduck, E.; Kasper, A.; Küstner, D.: Influence of raw materials and batch formula on the emission of flat glass tank furnaces. In: Mazurin, O. V. (ed.): Glass '89. Proc. XV International Congress on Glass, Leningrad 1989. Vol. 3a. Leningrad: Nauka, 1989. p. 179–184.
[37] Beek, A. P. M. ter; Thole, E. J. M. C.: Chloride emission from glass melting furnace. Glastech. Ber. **65** (1992) no. 11, p. 315–320.
[38] Beerkens, R. G. C.: Modeling the kinetics of volatilization from glass melts. To be published in J. Am. Ceram. Soc. 2001.
[39] Crank, J.: The mathematics of diffusion. Oxford : Clarendon, 1956. p. 34.
[40] Beerkens, R. G. C.: Heutige Möglichkeiten zur Modellierung von Glasschmelzöfen, Voraussagen zur Qualität des Glasschmelzprozesses. Glastech. Ber. Glass Sci. **71** (1998) no. 4, p. N35–N47.
[41] Lankhorst, A. M.; Muysenberg, H. P. H.; Sanders, M. J. P.: Coupled combustion modelling and glass tank modelling in oxy- and air-fired glass-melting furnaces. In: Proc. International Symposium on Glass Problems, Istanbul, 1996. Vol. 1. Instanbul, Sisecam, 1996. p. 378–384.
[42] Hermans, J.: Diffusion in glass melts. Eindhoven Univ. (The Netherlands), PhD thesis 2000. (In prep.)

0901P001

Addresses of the authors:

R. G. C. Beerkens
Eindhoven University of Technology
Department of Chemical Engineering and Chemistry
Laboratory for Chemical Reactor Engineering
P.O. Box 513
5600 MB Eindhoven
The Netherlands

J. van Limpt
TNO-TPD
P.O. Box 595
5600 AN Eindhoven
The Netherlands